Role of hybridization on the Schottky barrier height of carbon nanotube field effect transistors

D. Casterman and M. M. De Souza
Department of Electronic and Electrical Engineering, Mappin Building, Mappin Street, Sheffield S1 3JD, United Kingdom

A. Tahraoui, C. Durkan, and W. I. Milne
Department of Engineering, University of Cambridge, 9 J.J. Thomson Avenue, Cambridge CB3 0FA, United Kingdom
(Received 4 September 2008; published 5 March 2009)

The impact of hybridization on the Schottky barrier height (SBH) for holes at a metal/nanotube contact is investigated using *ab initio* density-functional theory. For small diameters, the impact of hybridization is a deviation of the SBH in comparison to that calculated using the "$1/d$" rule, where d is the diameter of the carbon nanotube (CNT). In the hybridization region, the SBH reduces with chiral angle, suggesting that CNTs in this region may well be suited to microelectronic applications due to small SBH and large band gaps. Hybridization also causes a difference between the effective mass of electrons and holes, supposed to be identical within the tight-binding approximation. A strongly patterned behavior of the effective mass dependent on chirality and diameter is also reported here.

DOI: 10.1103/PhysRevB.79.125407 PACS number(s): 85.35.−p, 61.48.De, 73.63.Fg

I. INTRODUCTION

Unlike conventional metal-oxide-semiconductor field effect transistors (FETs) (MOSFETs), carbon nanotube (CNT) field effect transistors (CNTFETs) have been demonstrated to operate either as Ohmic or Schottky barrier (SB) FETs.[1–4] Their observed sample-to-sample variation in current carrying capability is determined by the nature of the metallic electrode as well as diameter of the nanotube used as the channel.[2] Despite significant effort, no true value of the Schottky barrier height (SBH) has yet emerged.[2–4] This is largely due to the complexity associated with determining the physical structure of a CNT embedded in a CNTFET with bottom gate, whose drain current characteristics can also be measured nondestructively for the purpose of correlating the transport with the physical structure. Conventional techniques such as scanning probe microscopy (SPM) do not allow for measurement of tunneling current due to the presence of the bottom gate oxide. Atomic force microscopy (AFM) has an accuracy of $\pm 10\%$ but is incapable of resolution of nanotube chirality. Systematic Raman spectroscopy of single nanotubes embedded in a CNTFET is extremely challenging due to spot size of the spectroscope and the resolution of destructive methods such as high-resolution transmission electron microscopy (TEM) (HRTEM)/TEM is inversely proportional to the electron-beam energy. The difficulty in characterization has lead to different approaches to attempt extraction of the SBH from drain current characteristics of CNTFETs. In particular, Chen *et al.*[2] used a one-to-one comparison between experiment and simulation using statistical sampling to relate drain current characteristics measured for one set of devices with diameters determined via TEM from another set of devices. Kim *et al.*[3] and Tseng *et al.*[4] determined the diameters of each device using AFM and employed the model presented in Eq. (1) below to evaluate the barrier height. The Schottky barrier height is commonly required as input parameter to evaluate the transfer characteristic of CNTFETs via numerical simulations.[5,6]

Assuming the physical structure is known, the band structure can in principle be determined via calculations employing density-functional theory (DFT). However, such calculations suffer from limitations in modeling the exchange-correlation energy, whereas quasiparticle corrections to the band gap require prohibitive computing times even by modern standards, limiting the range of CNTs which can be explored. Despite these limitations, several *ab initio* DFT calculations have been reported on the impact of contact geometry and metal on the resistance.[7–11] These studies have revealed the superiority of the coupling of palladium with the nanotube in comparison to gold, for example, even though both metals possess similar work function. Strong perturbation of the nanotube electronic structure close to the metal interface may be expected particularly via metal induced gap states (MIGSs) which have been shown in several *ab initio* studies of metal/nanotube contacts.[9] The electrostatic dipole arising due to MIGs strongly affects the Schottky barrier height of the contact. Nonetheless, *ab initio* calculations which can examine this effect, particularly for chiral nanotubes, necessitate an excessive computational burden, which is beyond the scope of the present study. On the other hand, phenomenological models of the SB still retain their usefulness in assessment of device performance via transport calculations.[5,6,12] The SBH (for holes) can traditionally be expressed as the difference between the metal Fermi level E_F and the semiconducting valence-band edge E_v, given by

$$\Delta_0 = E_F - E_v = \frac{1}{2}E_G - \phi_M + \phi_{\mathrm{CNT}}, \tag{1}$$

where E_G is the band gap, Φ_{CNT} is the work function of the CNT, defined as the difference between the vacuum level (VL) and the Fermi level E_F, and Φ_M is the work function of the metal. Earlier models of the SBH rely on use of a conventional "$1/d$" dependence of the band gap of the CNT, derived from the tight-binding approximation[2,3,12] and on a constant work function Φ_{CNT}. Values of the proportionality constant in this relationship vary significantly in the literature as highlighted in Fig. 1, as indeed values of work function do (Φ_{CNT}=4.5 eV in Ref. 15 and 4.7 eV in Refs. 2 and

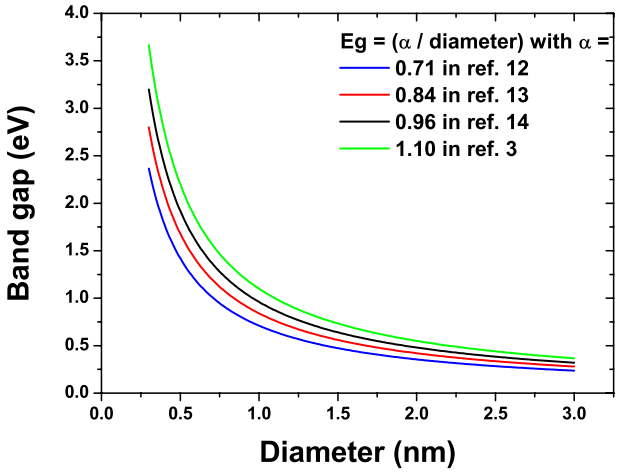

FIG. 1. (Color online) Variation of CNT band gap as a function of diameter. In this figure, the band gap is inversely proportional to the diameter but the coefficient of proportionality employed yields band gaps of 0.71 (Ref. 12), 0.84 (Ref. 13), 0.96 (Ref. 14), and 1.10 (Ref. 3) at 1 nm.

12), leading to widely varying values of the SBH. Using Eq. (1), Kim *et al.*[3] reported an ideal diameter value of ~1.8 nm whereas Tseng *et al.*[4] reported ideal diameters of 1.5 nm. In comparison to the simplistic model presented by Eq. (1), Leonard and Talin[12] developed an analytical model of the SB taking into account partial depletion of the nanotube at the nanoscale contact. This approach is reasonable since band bending at a metal-nanotube contact is expected to occur via charge transfer. Using this model, Leonard and Talin[12] reported an ideal diameter of 1.4 nm for Pd contacts. None of the above models include the impact of hybridization in their approach, though the impact of hybridization on the electronic band structure has first been reported by Blase *et al.*[16] and more recently by Zólyomi and Kürti[17] whereas that on the work function of the CNT was reported by Su *et al.*[18] A variation in the estimate of the ideal diameter for which the SBH is zero, described above, can be attributed to the uncertainty of these two parameters. The issue is relevant to the selection of appropriate semiconducting CNTs for microelectronic applications, i.e., those with large band gap but a zero SBH. Large diameter CNTs have smaller Schottky barriers,[2–4] but their band gaps are also smaller, leading to an increased ambipolar conduction and a poorer on/off ratio.

In this work, the impact of hybridization calculated via DFT on the SBH is evaluated using the Schottky barrier model for a partially depleted CNT. The impact of hybridization on the effective masses of electrons and holes is also demonstrated. This aspect is relevant in any approach which uses a comparison between measured and simulated drain characteristics to determine the SBH.[2] Electronic properties (band gap, work function) of the entire range of semiconducting (n,m)-CNTs with diameters from 0.4 to 1.6 nm, possible within supercell sizes of up to 200 atoms, are reported here. This work extends the data set of Zólyomi and Kürti[17] and Su *et al.*[18] and includes all of the above properties calculated within a single framework of simulation parameters. Additionally, the role of the chiral index for small diameter nanotubes in the determination of the SBH is highlighted. The *ab initio* calculated band structures are subsequently used to calculate the effective masses for holes and electrons and compared with those evaluated from tight binding.

II. METHOD

Calculations were carried out using DFT implemented in the Vienna *Ab initio* Simulation Package (VASP).[19–22] In the present calculations, an ultrasoft pseudopotential[23,24] was employed to describe the interaction between the ions and the valence electrons together with the local-density approximation (LDA) to model the exchange-correlation energy.[25] The cutoff energy was chosen to be equal to ~360 eV which is sufficient to obtain well converged results within this framework. All structures were relaxed using three-dimensional (3D) periodic boundary conditions in large supercells of length equal to the translational vector along the nanotube and at least 10 Å of vacuum in the other directions until the forces acting on each atom decreased below 0.005 eV/atom. The Monkhorst-Pack technique centered at Γ with appropriate meshes (depending on the length of the translational vector of the nanotube) was used for the integration over the first Brillouin zone[26] and a Gaussian method with a smearing width of 0.1 eV was used for smoothing of the density of states near the Fermi level.

III. RESULTS

The calculated electronic properties have been summarized in Table I. Figure 2 represents the variation in the work function and band gap as a function of diameter. The work function is shown to increase while the band gap decreases with reduction in diameter due to hybridization, and the reported values are consistent with previous theoretical investigations.[17,18,27] The deviation of the band gap from the $1/d$ rule, highlighted by the dashed line in Fig. 2, is more prominent for small chiral angles. To evaluate the impact of these properties on the SBH, the electrostatic potential and the charge density are solved self-consistently using Eqs. (2) and (3) given below for clarity,

$$\sigma = qN\left\{\int_{-\infty}^{E_v - qV_{\mathrm{NT}}} [1 - f(E)]D(E + qV_{\mathrm{NT}})dE - \int_{E_c - qV_{\mathrm{NT}}}^{\infty} f(E)D(E + qV_{\mathrm{NT}})dE\right\}, \tag{2}$$

$$V_{\mathrm{NT}} = \frac{\sigma R}{\varepsilon_0}\ln\left(\frac{R+s}{R}\right). \tag{3}$$

In Eq. (2), R is the carbon nanotube radius, s is the distance between the nanotube and the metal (and is equal to 3 Å in this work), $f(E) = 1/[1+e^{(E-E_F)/k_BT}]$ is the Fermi-Dirac distribution, E_F is the Fermi level, and $D(E+eV_{\mathrm{NT}})$ is the density of states shifted by the electrostatic potential V_{NT} determined

TABLE I. Summary of the electronic properties calculated from *ab initio* calculations. In this table, the diameter is given in nm, the band gap Eg and the work function Φ_{CNT} are given in eV, and the effective masses for holes (m_h) and electrons (m_e) are given as a fraction of the free-electron mass (m_0).

Diameter (nm)	Chirality (n,m)	Translational vector (nm)	Eg (eV)	Φ_{CNT} (eV)	m_h/m_0	m_e/m_0
0.41	(4,2)	1.13	0.27	5.14	0.43	0.20
0.44	(5,1)	2.37	0.04	5.17	0.10	0.17
0.48	(4,3)	2.59	1.33	4.72	0.18	0.18
0.51	(6,1)	2.79	0.42	4.98	0.41	0.16
0.55	(5,3)	2.98	1.20	4.62	0.24	0.21
0.55	(7,0)	0.43	0.28	5.02	0.1	0.16
0.57	(6,2)	1.54	0.69	4.77	0.11	0.18
0.62	(8,0)	0.43	0.55	4.78	0.27	0.17
0.68	(6,4)	1.86	1.09	4.58	0.17	0.18
0.78	(10,0)	0.43	0.86	4.6	0.09	0.09
0.83	(8,4)	1.13	0.81	4.55	0.11	0.10
0.86	(11,0)	1.13	0.83	4.52	0.16	0.16
1.02	(13,0)	0.43	0.72	4.58	0.07	0.07
1.04	(10,5)	0.43	0.74	4.52	0.13	0.12
1.10	(14,0)	0.43	0.72	4.51	0.14	0.19
1.25	(16,0)	0.43	0.62	4.57	0.07	0.07
1.33	(17,0)	0.43	0.49	4.55	0.08	0.08
1.57	(20,0)	0.43	0.50	4.52	0.10	0.12

by solving the Poisson equation [Eq. (3)] in a cylindrical geometry. The SBH for holes (Δh) and electrons (Δe) is determined by Eqs. (4) and (5),

$$\Delta h(d) = E_f^{\text{metal}} - E_v^{\text{CNT}} = \Delta h_0(d) + qV_{\text{NT}} = \left\{ \frac{Eg(d)}{2} - [\phi_m - \phi_{\text{CNT}}(d)] \right\} + qV_{\text{NT}}, \quad (4)$$

$$\Delta e(d) = E_c^{\text{CNT}} - E_f^{\text{metal}} = \Delta e_0(d) - qV_{\text{NT}} = \left\{ \frac{Eg(d)}{2} + [\phi_m - \phi_{\text{CNT}}(d)] \right\} - qV_{\text{NT}}, \quad (5)$$

where $\Delta h_0(d)$ and $\Delta e_0(d)$ are the SBHs before charge transfer and $\Delta h(d)$ and $\Delta e(d)$ are the SBHs which take partial depletion into account.

From these equations, the SBH for holes, as a function of diameter, for the same three metals examined by Chen *et al.*[2] [palladium (Φ_{Pd}=5.1 eV), titanium (Φ_{Ti}=4.3 eV), and aluminum (Φ_{Al}=4.1 eV)] using DFT calculations (dots) is compared with that obtained using the "$1/d$ rule" (lines) as described in Fig. 3(a) of Ref. 28. This figure indicates a Schottky contact for holes using titanium and aluminum and a transition from Schottky to Ohmic contact using palladium as observed experimentally.[2] At diameters smaller than 0.8 nm, hybridization results in an even greater reduction in the SB via an increase in the work function and reduction in the band gap. The deviation from the traditional picture in the small diameter region observed in Fig. 3(a) can account for the deviation observed experimentally by Chen *et al.* (see Figs. 2 and 3 of Ref. 2), related at the time to the reactive nature of the contact. Larger deviations observed for titanium and aluminum in comparison to palladium are also consistent with experiment.

The diameter at which the contact varies from Schottky to Ohmic (between 0.9 and 1 nm) is lower than the diameter

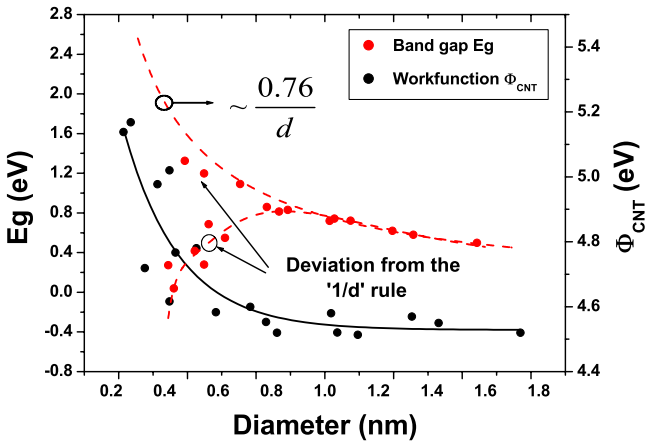

FIG. 2. (Color online) Variation in the band gap (dashed line) and work function (full line) with the diameter, d, of the CNT, calculated via DFT. The empty and full circles represent the band gap and work function, respectively. The dotted line indicates inverse dependence of diameter with a proportionality factor of 0.76. However, a deviation from this $1/d$ rule is observed due to hybridization for diameters less than 0.8 nm.

determined experimentally (about 1.3–1.4 nm). This may be explained by several factors: the constant in the $1/d$ relationship from our DFT calculations is about 0.76 whereas Chen *et al.*[2] used a value of about 0.84 and the work function of CNT of about 4.7 eV in comparison to the present values. Finally, the reduction in band gap within DFT is another important consideration.

Figure 3(b) represents the variation in the SBH for holes as a function of the chiral angle θ of CNTs for diameter of 0.5 nm. The energy barrier is seen to increase as θ approaches $\pi/6$ even though this effect is small for palladium due to the weak variation in the SBH with θ in this metal. The y axis in Fig. 3(b) is representative of the error bar associated with the value of SB for one given diameter. The significant variation in SBH with chirality explains some of the variations observed from device to device even for the same diameter nanotubes.[2,4] These results are indicative of the fact that small diameter CNTs having small chiral angles may well possess negligible SB and reasonable band gaps for microelectronic applications, though practical considerations may include the ability to achieve Ohmic contacts for such small diameters.

The effective masses are determined from the band structure calculated within VASP by fitting the electronic bands and calculated from a tight-binding band structure as presented in Eq. (6),[29,30]

$$E(k) = \pm\gamma_0 \sqrt{\begin{array}{l} 1 + 2\cos\left(\dfrac{akm\sqrt{3}}{2\sqrt{m^2+nm+n^2}} + \dfrac{q\pi(m+2n)}{m^2+nm+n^2}\right) \\ +2\cos\left(-\dfrac{akn\sqrt{3}}{2\sqrt{m^2+nm+n^2}} + \dfrac{q\pi(2m+n)}{m^2+nm+n^2}\right) \\ +4\cos^2\left(\dfrac{ak(m+n)\sqrt{3}}{4\sqrt{m^2+nm+n^2}} + \dfrac{q\pi(n-m)}{2(m^2+nm+n^2)}\right) \end{array}} = \pm\gamma_0\sqrt{u(k)} \tag{6}$$

where γ_0 is the transfer integral between the π orbitals of neighboring atoms (equal to 2.5 eV in this work), k is the wave number, and q defines the allowed lines for $\mathbf{k}$. Using these notations, the effective masses are given by

$$\frac{m_{h,e}}{m_0} = \frac{\hbar^2}{m_0 \left.\dfrac{\partial^2 E(k)}{\partial k^2}\right|_{k=k_0}} = \frac{2\sqrt{u(k_0)}\hbar^2}{m_0\gamma_0\left[\left.\dfrac{\partial^2 u(k)}{\partial k^2}\right|_{k=k_0} - \dfrac{1}{2}\left(\left.\dfrac{\partial u(k)}{\partial k}\right|_{k=k_0}\right)^2 \dfrac{1}{u(k_0)}\right]}. \tag{7}$$

The calculated masses have been summarized in Table I. Some of these values are in good agreement with those found in Ref. 27. However, a more complete set of masses is presented in Fig. 4(a) as a function of the diameter. For clarity, only the masses of holes have been plotted in this figure. Clear patterns appear in the variation in these masses and bear full agreement with the patterns observed in the adsorption-emission spectra of previous spectrofluorimetric measurements on single-walled carbon nanotubes isolated in aqueous surfactant suspensions.[31] The first pattern is associated with the "family pattern" and is denoted F_i (with $i \in [1,\ldots,5]$) in Fig. 4(a). These curves, F_i, are "exponentially" decaying and link the masses of all (n,m)-CNTs having the same property $n-m=i$ [e.g., F_1 corresponds to the family (3,2)-, (4,3)-, (5,4)-, …, (18,17)-CNTs]. The second pattern, also known as the $2n+m=$const family,[32] corresponds to the transversal lines [see gray thick lines in Fig. 4(a) which connect the masses of all the (n,m)-CNT whose chiral indices vary "either by -1 in the value of n and $+2$ in m or $+2$ in n and -1 in m"]. For example, one of these transversal lines is shown to link the (7,0)-, (6,2)-, (5,4)-, (6,4)-, (8,3)-, (10,2)-, (12,1)-, and (14,0)-CNTs. Whereas the variation in the electronic band gap is mainly dependent of the diameter, the effective masses of electrons and holes highlight the uniqueness of each carbon nanotube in the same manner as the variation in phonon frequency[33] and photoluminescence excitation-emission spectra[31] with chirality and diameter, which are essential in separation and purification techniques.

Beyond this picture described within the tight-binding approximation, Fig. 4(b) presents the variation in the effective masses of holes evaluated from the present *ab initio* calculations. The dotted lines represent to some extent the patterns described above. In this figure, hybridization appears to open up the shape described by the variation in the effective masses of holes in the tight-binding approximation, whereas the effective mass of the large diameter CNTs is in good agreement with those calculated from tight binding.

Moreover, in contrast to the masses of holes, electron masses appear to approach a constant value ranging between $0.15m_0$ and $0.20m_0$ as the diameter decreases (see Table I). This discrepancy between the masses of electrons and holes

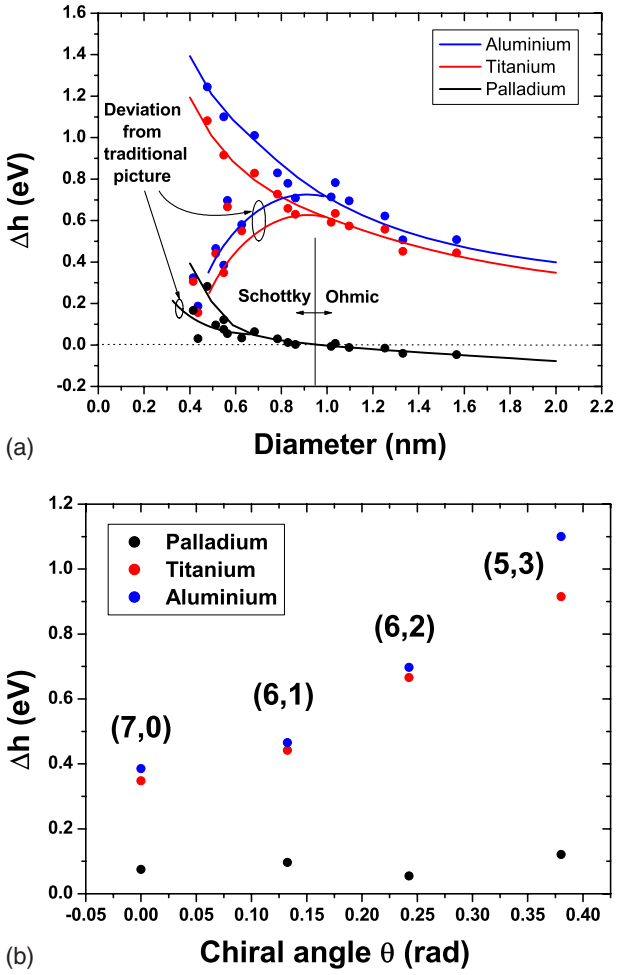

FIG. 3. (Color online) (a) Variation in the SBH for holes, Δh, as a function of the CNT diameter. In these figures, the dots and the lines, respectively, represent the SBH calculated from the electronic properties extracted from *ab initio* calculations and from the traditional picture (band gap inversely proportional to the diameter and constant work function). (b) represents the variation in the SBH for holes as a function of the chiral angle, θ, of CNTs having a diameter of ~0.5 nm.

is highlighted in Fig. 4(c) which represents the ratio between both sets of masses. In the hybridization region, the ratio largely differs from the ideal limit 1 which reflects the mirror image of the valence and conduction bands in the tight-binding approximation. The values of the effective mass are particularly important for the evaluation of the Schottky barrier height from a one-to-one comparison between experiment and simulation as in Ref. 2.

IV. CONCLUSION

In conclusion, the results presented in this work demonstrate the importance of the individual contribution of the electronic band gap and work function of the nanotube at small diameters in the evaluation of the SBH. This qualitative approach used in the evaluation of SBH highlights its dependence on both the diameter and chirality. These results based on density-functional theory show a deeper insight in

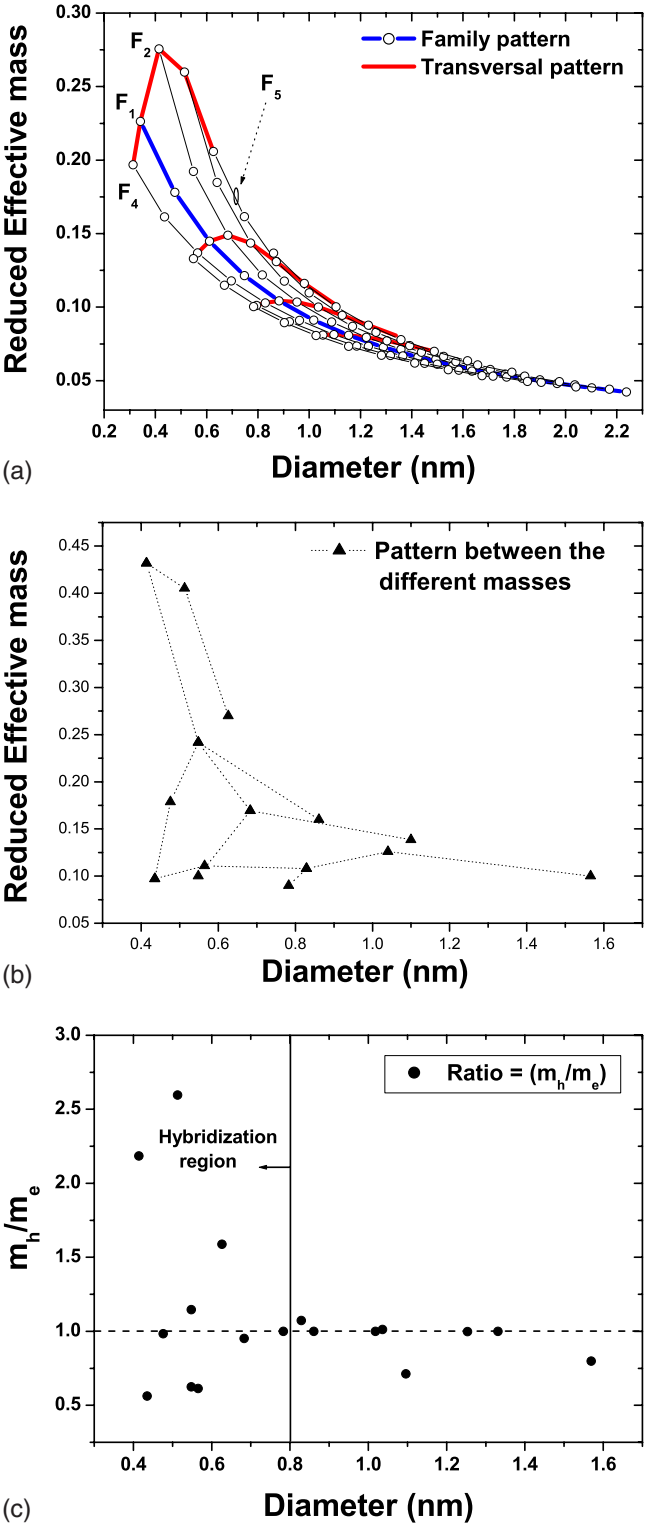

FIG. 4. (Color online) Variation in the calculated effective masses for holes as a function of the diameter. (a) represents the effective masses calculated from the tight-binding approximation and (b) from *ab initio* calculations. For both figures, each intersection point corresponds to a particular chirality and the lines correspond to the patterns observed. (c) Variation in the ratio between the masses of holes and electrons estimated via *ab initio* calculations. The dashed line corresponds to the ratio of these masses within tight-binding approximation, i.e., equal to 1.

selecting an appropriate choice of CNTs for microelectronic applications. However, this analysis does not take into account the effect of metal induced gap states at the metal-CNT contact which plays an important role in the quantitative determination of the Schottky barrier.

ACKNOWLEDGMENTS

This work, as part of the European Science Foundation EUROCORES Programme FoNE, was supported by funds from the EPSRC and the EC Sixth Framework Programme under Contract No. ERAS-CT-2003-980409.

[1] A. Javey, J. Guo, Q. Wang, M. Lundstrom, and H. Dai, Nature (London) **424**, 654 (2003).
[2] Z. Chen, J. Appenzeller, J. Knock, Y. L. Lin, and Ph. Avouris, Nano Lett. **5**, 1497 (2005).
[3] W. Kim, A. Javey, R. Tu, and H. Dai, Appl. Phys. Lett. **87**, 173101 (2005).
[4] Y. C. Tseng, K. Phoa, D. Carlton, and J. Bokor, Nano Lett. **6**, 1364 (2006).
[5] J. Guo, S. Datta, and M. Lundstrom, IEEE Trans. Electron Devices **51**, 172 (2004).
[6] K. Alam and R. K. Lake, J. Appl. Phys. **98**, 064307 (2005); **100**, 024317 (2006).
[7] B. Shan and K. Cho, Phys. Rev. B **70**, 233405 (2004).
[8] J. J. Palacios, A. J. Perez-Jimenez, E. Louis, E. San Fabian, and J. A. Verges, Phys. Rev. Lett. **90**, 106801 (2003).
[9] J. J. Palacios, P. Tarakeshwar, and D. M. Kim, Phys. Rev. B **77**, 113403 (2008).
[10] N. Nemec, D. Tomanek, and G. Cuniberti, Phys. Rev. Lett. **96**, 076802 (2006).
[11] W. Zhu and E. Kaxiras, Nano Lett. **6**, 1415 (2006).
[12] F. Leonard and A. A. Talin, Phys. Rev. Lett. **97**, 026804 (2006), arXiv:cond-mat/0602003.
[13] A. Javey, M. Shim, and H. Dai, Appl. Phys. Lett. **80**, 1064 (2002); M. Pourfath, E. Ungersboeck, A. Gehring, W. J. Park, B. H. Cheong, H. Kosina, and S. M. Selberherr, Microelectron. Eng. **81**, 428 (2005).
[14] H. Dai, A. Javey, E. Pop, D. Mann, and Y. Lu, NANO **1**, 1 (2006).
[15] D. L. John, L. C. Castro, J. Clifford, and D. L. Pulfrey, IEEE Trans. Nanotechnol. **2**, 175 (2003).
[16] X. Blase, L. X. Benedict, E. L. Shirley, and S. G. Louie, Phys. Rev. Lett. **72**, 1878 (1994).
[17] V. Zólyomi and J. Kürti, Phys. Rev. B **70**, 085403 (2004).
[18] W. S. Su, T. C. Leung, and C. T. Chan, Phys. Rev. B **76**, 235413 (2007).
[19] G. Kresse and J. Hafner, Phys. Rev. B **47**, 558 (1993).
[20] G. Kresse and J. Hafner, Phys. Rev. B **49**, 14251 (1994).
[21] G. Kresse and J. Furthmüller, Comput. Mater. Sci. **6**, 15 (1996).
[22] G. Kresse and J. Furthmüller, Phys. Rev. B **54**, 11169 (1996).
[23] D. Vanderbilt, Phys. Rev. B **41**, 7892 (1990).
[24] G. Kresse and J. Hafner, J. Phys.: Condens. Matter **6**, 8245 (1994).
[25] J. P. Perdew and A. Zunger, Phys. Rev. B **23**, 5048 (1981).
[26] H. J. Monkhorst and J. D. Pack, Phys. Rev. B **13**, 5188 (1976).
[27] G. L. Zhao, D. Bagayoko, and L. Yang, Phys. Rev. B **69**, 245416 (2004).
[28] We refer as "$1/d$ rule" the fact to consider the band gap inversely proportional to the diameter and the work function constant in a CNT. These models were often used in recent years to explain experimental and theoretical results.
[29] J.-C. Charlier, X. Blase, and S. Roche, Rev. Mod. Phys. **79**, 677 (2007).
[30] J. M. Marulanda and A. Srivastava, Phys. Status Solidi B **245**, 2558 (2008).
[31] S. Bachilo, M. S. Strano, C. Kittrell, R. H. Hauge, R. E. Smalley, and R. B. Weisman, Science **298**, 2361 (2002).
[32] G. Samsonidze, R. Saito, N. Kobayashi, A. Grüneis, J. Jiang, A. Jorio, S. G. Chou, G. Dresselhaus, and M. S. Dresselhaus, Appl. Phys. Lett. **85**, 5703 (2004).
[33] H. Wang, X. Cao, M. Feng, Y. Wang, Q. Jin, D. Ding, and G. Lan, Spectrochim. Acta, Part A **71**, 1932 (2009).